Modelling of accelerograms of two Himalayan earthquakes using a novel semi-empirical method and estimation of accelerogram for a hypothetical great earthquake in the Himalaya

Dinesh Kumar, K. N. Khattri*, S. S. Teotia and S. S. Rai[†,§]

Department of Earth Sciences, Kurukshetra University, Kurukshetra 136 119, India
*100, Rajindra Nagar, Kaulagarh Road, Dehradun 248 001, India
[†]National Geophysical Research Institute, Uppal Road, Hyderabad 500 007, India

This paper presents a fast semi-empirical method for calculating synthetic accelerograms for a wide range of earthquake magnitudes. The fidelity of this method is demonstrated by successful modelling of the observed accelerograms of the 1986 Dharmsala (M_s 5.3) and the 1991 Uttarkashi (M_s 7) earthquakes at relatively shorter distances. At larger distances, the synthetic accelerograms tend to over-estimate the ground motions. The method has also been tested for a hypothetical great earthquake (M_w 8.5) by comparing the synthetic accelerogram with that obtained using the more sophisticated composite source model. The method has applications where seismic hazard needs to be estimated and empirical data sets including accelerograms, velocity-Q models and earthquake focal mechanisms are sparse or not available at all. It will also be useful in obtaining uniform probability response spectra for such regions.

THE design of appropriate preventive measures to minimize disasters from earthquakes is dependent on the proper evaluation of the seismic hazard in the region. The source of damage lies most often with the strong shaking caused by the waves set up by the earthquakes. The records of strong ground motions from past earthquakes can serve to provide a wealth of information that will be indispensable in the design of earthquake-resistant structures. In many regions like the Himalaya, such records generated by past earthquakes are few or absent and one needs to use theoretical formulations to estimate accelerograms from expected earthquakes in order to assess the seismic hazard. A number of techniques have been proposed to simulate the strong ground motions. These include: (1) Auto regressive moving average (ARMA) methods[1–3], which simulate the ground acceleration time-history by a multistep discrete equation. The basic deficiency of such methods is that the physical interpretation of the coefficients in the generating equation is not directly obvious[4]. (2) Composite source model[5–7] in which synthetic accelerograms are calculated by modelling the features of earthquake source process and using wave propagation theory. This method has proved to be quite successful in representing the empirical strong ground motions. However, one requires the velocity-Q structure of the region as well as the fault plane solution of the earthquake and the stress drop parameter. Also, calculation of the complete Green's functions is quite time-intensive. (3) Empirical Green's function approach to synthesize the strong ground motions[8–14] which is advantageous in the sense that it takes into account the complexity of heterogeneous structures between the source and the observation site. However, the small event record, foreshock or aftershock (empirical Green's function), from the source region of the main earthquake may not be available for the site of interest.

Midorikawa[15] proposed a method based on the semi-empirical method of Irikura[9] for estimating the peak ground acceleration created by larger earthquakes from those of smaller ones. He obtained the envelope of the larger earthquake by superposing the envelopes of the accelerograms of smaller earthquakes and used it to estimate the expected peak ground acceleration due to the larger earthquake.

We present and use here a fast semi-empirical method first proposed by Khattri[16] for obtaining synthetic accelerograms for large earthquakes. This method is an extension of the Midorikawa[15] procedure illustrating the fidelity of the method by modelling a few accelerograms recorded for the 1986 Dharmsala and the 1991 Uttarkashi earthquakes. We use this method for modelling of all the accelerograms for the 1986 Dharmsala and the 1991 Uttarkashi earthquakes. We also compare the accelerogram for a hypothetical M_w 8.5 earthquake obtained using this method with the accelerogram obtained using the composite source model.

Technique

For the purpose of simulating accelerograms caused by a large earthquake we represent its anticipated rupture

[§]For correspondence. (e-mail: postmast@csngri.ren.nic.in)

surface by a rectangular plane. The fault plane is divided into $n \times n$ elements[9]. The size of each element corresponds to a small earthquake, the record of which is used as an empirical Green's function. n is a scaling parameter given by the following relation[15].

$$n = 10^{0.5(M-M')}, \tag{1}$$

where M and M' are the magnitudes of the large and small earthquake respectively. As the appropriate empirical Green's functions are not available for all the sites, Midorikawa[15] proposed the use of the envelope waveform, instead of the actual time-history, corresponding to each element of the fault plane. He adopted the following envelope function used by Kameda and Sugito[17] to simulate the peak acceleration from large earthquakes:

$$e_{ij}(t) = (a_{ij}t/d_{ij})^{*}\exp(1 - t/d_{ij}) \tag{2}$$

where $e_{ij}(t)$ is the envelope function corresponding to the (i, j)th element of the fault plane. a_{ij} and d_{ij} are the peak acceleration and duration parameters respectively, determined from the existing empirical relations for these parameters, t is the time.

The acceleration envelope waveform $\hat{e}(t)$ of the large earthquake (target earthquake) can be synthesized by the summation of the envelope, $e_{ij}(t)$ as follows[15]:

$$\hat{e}(t) = \left[\sum_i \sum_j e_{ij}(t - t_{ij})\right]^{1/2}, \tag{3}$$

where t_{ij} is the time delay due to rupture propagation and travel time of seismic waves.

In order to simulate the earthquake accelerograms due to the target (larger) earthquake, the envelope waveform generated by eq. (3) above is next multiplied with a band limited normalized white noise (representing acceleration) to produce the desired accelerogram. The low-cut frequency of the band limited white noise is chosen to correspond to the corner frequency for the target earthquake magnitude and the high-cut to Boore's f_{max} or a desired frequency for the simulation. Below the low-cut frequency, the fall-off slope is 2 in accordance with the w^2 earthquake source model. The various steps for synthesizing accelerograms using the proposed method are shown in Figure 1.

Using the method described above, we have computed accelerograms of the 1986 Dharmsala earthquake (5.3 M_s) at 9 sites and of the 1991 Uttarkashi earthquake (7 M_s) at 13 sites. The synthetic accelerograms and the observed accelerograms have been compared in terms of peak ground acceleration values, waveforms, Fourier spectra and response spectra visually.

In addition, the root mean square error (rmse) between the synthetic and observed response spectra has also been calculated as a measure of goodness of fit using the following equation

$$\text{rmse} = [(1/N)\,\Sigma\{(R_{obs} - R_{cal})/R_{obs}\}^2]^{1/2}, \tag{4}$$

where R_{obs} and R_{cal} are the observed and calculated response spectra respectively. In addition, we have

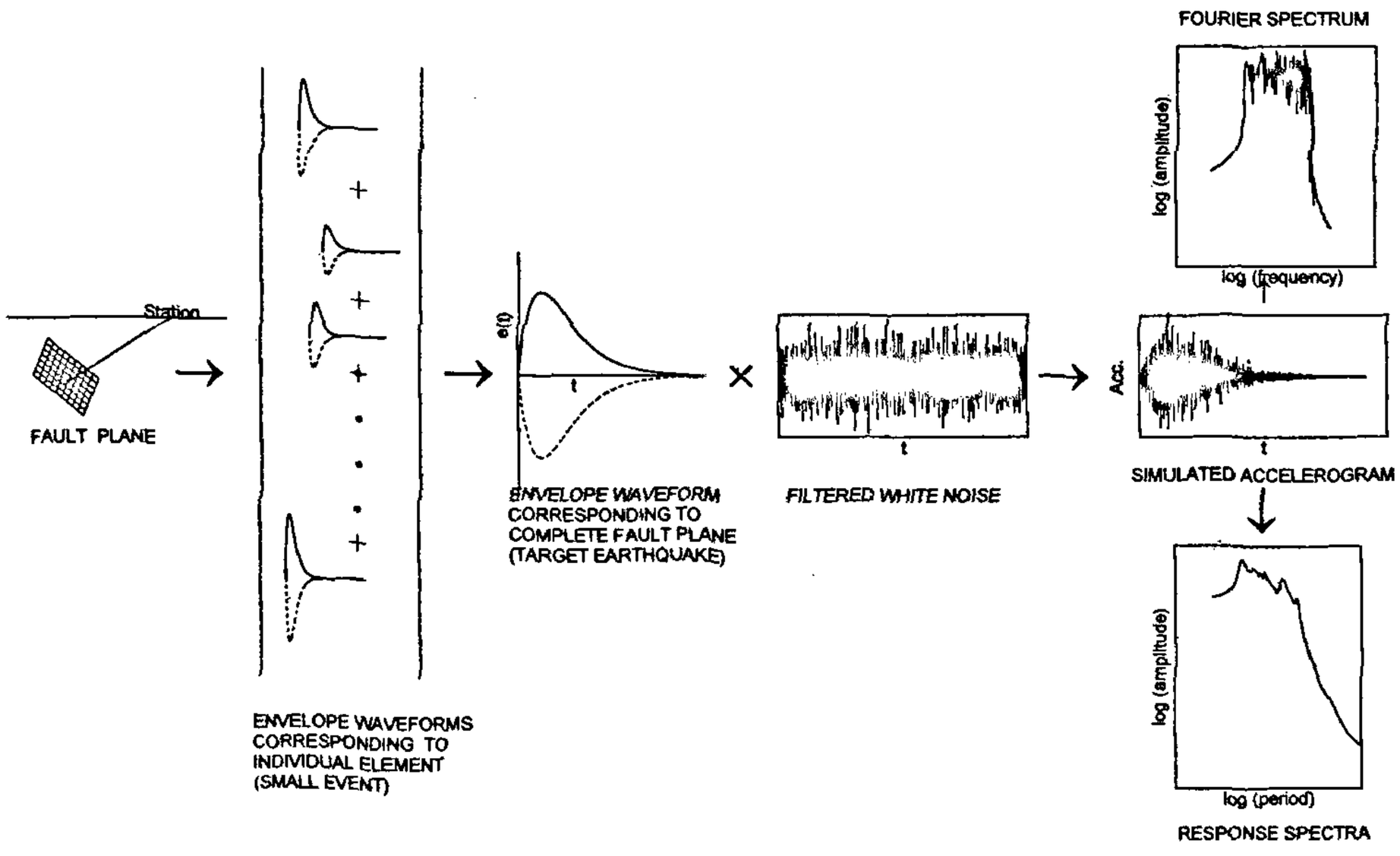

Figure 1. Schematic illustration of various steps for synthesizing accelerograms using the proposed method.

synthesized the accelerogram for a hypothetical great earthquake in the Himalaya and compared the results with those obtained using the composite source model.

The advantage of the proposed semi-empirical technique is that it is very fast to calculate and is based on simple empirical relations. It neither requires the actual records of a small event as in the case of empirical Green's function technique nor the velocity-Q structure, the fault plane solution and stress drop parameter as in the case of the composite source model.

Empirical relations for peak acceleration and duration parameter

In order to compute the envelope waveform corresponding to the elements on the fault plane using eq. (2), the peak acceleration (a_{ij}) and the duration parameter (d_{ij}) need to be determined. The peak acceleration is determined from the attenuation relation for the region where the envelope waveform due to a large earthquake is required. The seismo-tectonic regions are characterized by their specific attenuation relations. In the Himalaya, the data sets obtained thus far are not adequate to allow multiple regression analysis for obtaining attenuation relations for various sectors. Therefore, to apply the semi-empirical technique discussed here for the earthquakes in the Himachal and Garhwal Himalaya sectors, we have adopted from the various available attenuation relations the one which gives the best fit to the observed data. It has been found that the Dharmsala and Uttarkashi areas which lie in adjacent sectors of the Himalaya have different attenuation characteristics. The attenuation relation of Peng *et al.*[18] for China describes the Dharmsala earthquake data set relatively well and that of Abrahamson and Litehiser[19] is capable of satisfactorily predicting the Uttarkashi data set[20]. Accordingly, we have adopted the following relation[18] for the peak acceleration parameter for the 1986 Dharmsala earthquake:

$$\log(a) = 0.437 + 0.454\, M_s - 0.739 \log(r) - 0.00279r,$$

where a is the acceleration in cm/s^2, M_s is the earthquake surface wave magnitude and r is the epicentral distance in km.

For the 1991 Uttarkashi earthquake, the following relation[18] has been adopted:

$$\log(a) = -0.62 + 0.177\, M_s - 0.982 \log(R + \exp(0.284\, M_s)) + 0.132F - 0.0008ER,$$

where a is the acceleration in g, M_s is the earthquake surface wave magnitude and R is the hypocentral distance in km. F is 1 for reverse fault and 0 otherwise. E is a parameter equal to 1 for interplate and 0 for intraplate events.

We have used the above relation for the hypothetical event also as the earthquake lies in the same region as the Uttarkashi earthquake.

We have modified the duration parameter relation from that defined by Midorikawa[15] in order to conform to the empirical observations in the case of the Dharmsala earthquake:

$$d = 0.015*10^{0.05M'} + 0.12x^{0.75},$$

where d is the duration parameter, M' is the earthquake magnitude of the small event, x is the distance (in km) of the element from the site.

Strong motion data sets

The hypocentral parameters of the 1986 Dharmsala earthquake are as follows[21]: Latitude, 32.175°N; longitude, 76.287°E; depth, 7 km.

Figure 2 shows the location of the 1986 Dharmsala earthquake and the recording stations along with main tectonic features of the region.

The location of the 1991 Uttarkashi earthquake of magnitude 7 M_s is as follows (PDE, October, 1991): latitude: 30.780°N, longitude: 78.774°E, depth: 10 km.

Figure 3 shows the location of the 1991 Uttarkashi earthquake along with the 13 recording stations. The surface projection of the fault plane is also shown in the figure.

Results

1986 Dharmsala earthquake

Because of its small magnitude, the fault plane is considered as a single element. The corner frequency of 1 Hz has been taken in accordance with the magnitude of the earthquake. The highest frequency adopted in the synthetic accelerograms is 10 Hz. This choice is based on the consideration that most housing have resonant frequencies less than 5 Hz. Therefore for proper comparison, the observed accelerograms have also been bandpass-filtered to the same frequency band. The frequency-dependent attenuation during propagation, which modifies the spectral shape of the wave field as a function of distance is taken into account by using the following relation for Q (ref. 22):

$$Q(f) = 126f^{0.95},$$

where f is the frequency in Hz. The attenuation is given by

$$A_s(f) = A_0(f)e^{-\pi fR/Q\beta},$$

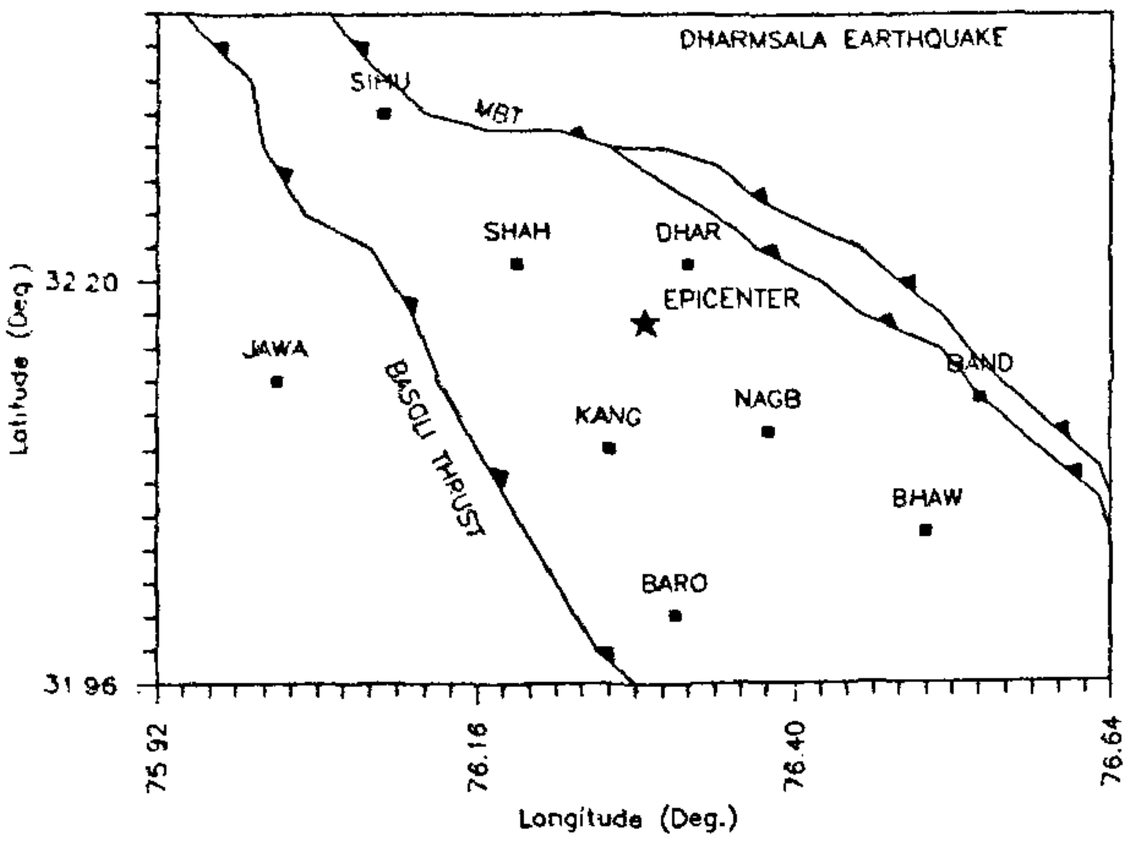

Figure 2. Location of the 1986 Dharmsala earthquake and recording stations along with main tectonic features of the region.

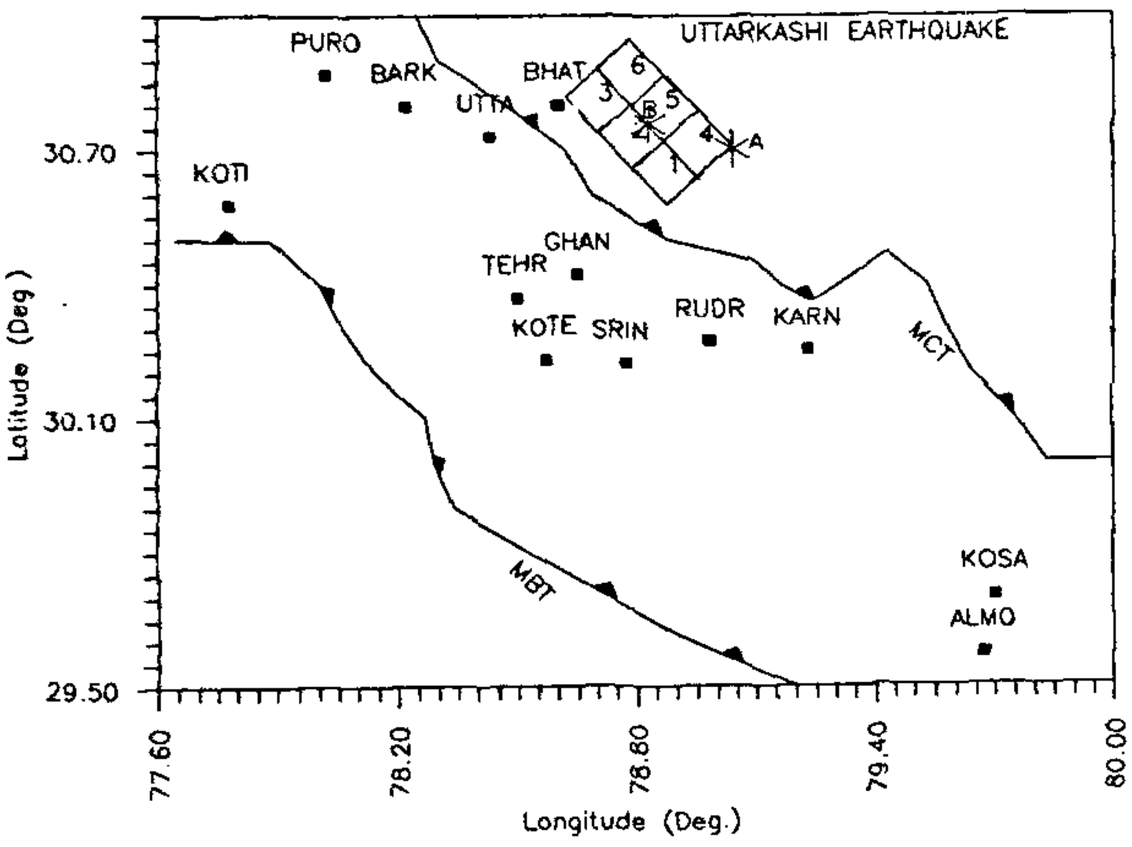

Figure 3. Location of the 1991 Uttarkashi earthquake and recording stations. The surface projection of the fault plane is also shown. The numbers on the fault plane indicate the element number (see text).

where $A_x(f)$ and $A_0(f)$ are spectral amplitudes at distance x and 0 respectively, f is the frequency, R is the distance, Q is the attenuation factor and β is the velocity.

Figure 4 shows the simulated accelerograms, the envelope functions, the L and T horizontal components of recorded accelerograms, the corresponding Fourier spectra and response spectra (5% damping). The continuous lines in the Fourier and response spectra correspond to the simulated accelerograms, while the long dash and small dash lines correspond to the transverse and longitudinal components of the recorded accelerograms.

The simulated acceleration time-histories are in agreement with those recorded in terms of frequency content and duration of strong shaking at almost all the stations. The relatively better matches are for the Dharmsala, Kangra, the T components of the Shahpur, Bandlakhas and the L components of Nagrota–Bagwan and Baroh stations. At other stations the matching is poor. This is particularly so for distant stations where the empirical accelerograms are significantly weaker than the synthesized ones.

The degree of match may also be compared in the Fourier and the response spectral domains. The comparison as seen in the response spectra is quite satisfactory at Dharmsala, Kangra, Nagrota–Bagwan, and Baroh. At Shahpur and Bandlakhas the quality of matching is satisfactory for long periods than for short periods where the synthetics are weaker than the empirical response curves. At Sihunta and Bhawarna, the matching is less satisfactory where the empirical response curves are weaker than the synthetics. At Jawali, the synthetic response spectrum is stronger than that of the observed one. This may be expected from the observed accelerograms as well. The above observations are reflected in the Fourier spectra also although due to roughness of the same the comparisons become fuzzy. Table 1 shows the rmse of the synthetic with the observed response spectra.

The graph of peak ground acceleration versus distance is shown in Figure 5. The values for the synthetic accelerograms are shown by plus signs and the empirical values are shown by circles. The curve shows the relation of Peng *et al.*[17] used in the analysis. The peak values of the present analysis are falling on the curve as expected.

1991 Uttarkashi earthquake

This event being larger in magnitude, has to be modelled by a larger fault area consisting of 22 × 36 sq km. Six elemental earthquakes each having a magnitude (M_s) of 6.2 are superposed as shown in Figure 3. The epicenter may be appropriately chosen. We have experimented with the epicenter at the NE corner (A) in congruity with

Table 1. The rms error of synthetic with observed (T and L components) response spectra for 1986 Dharmsala earthquake

Up to → Station	1s T	1s L
Dharmsala	0.68	1.70
Kangra	0.49	0.60
Shahpur	0.54	0.75
Nagrota–Bagwan	2.20	0.39
Baroh	1.04	0.62
Sihunta	0.97	0.90
Bandlakhas	0.52	0.54
Bhawarna	1.30	2.30
Jawali	3.10	3.00

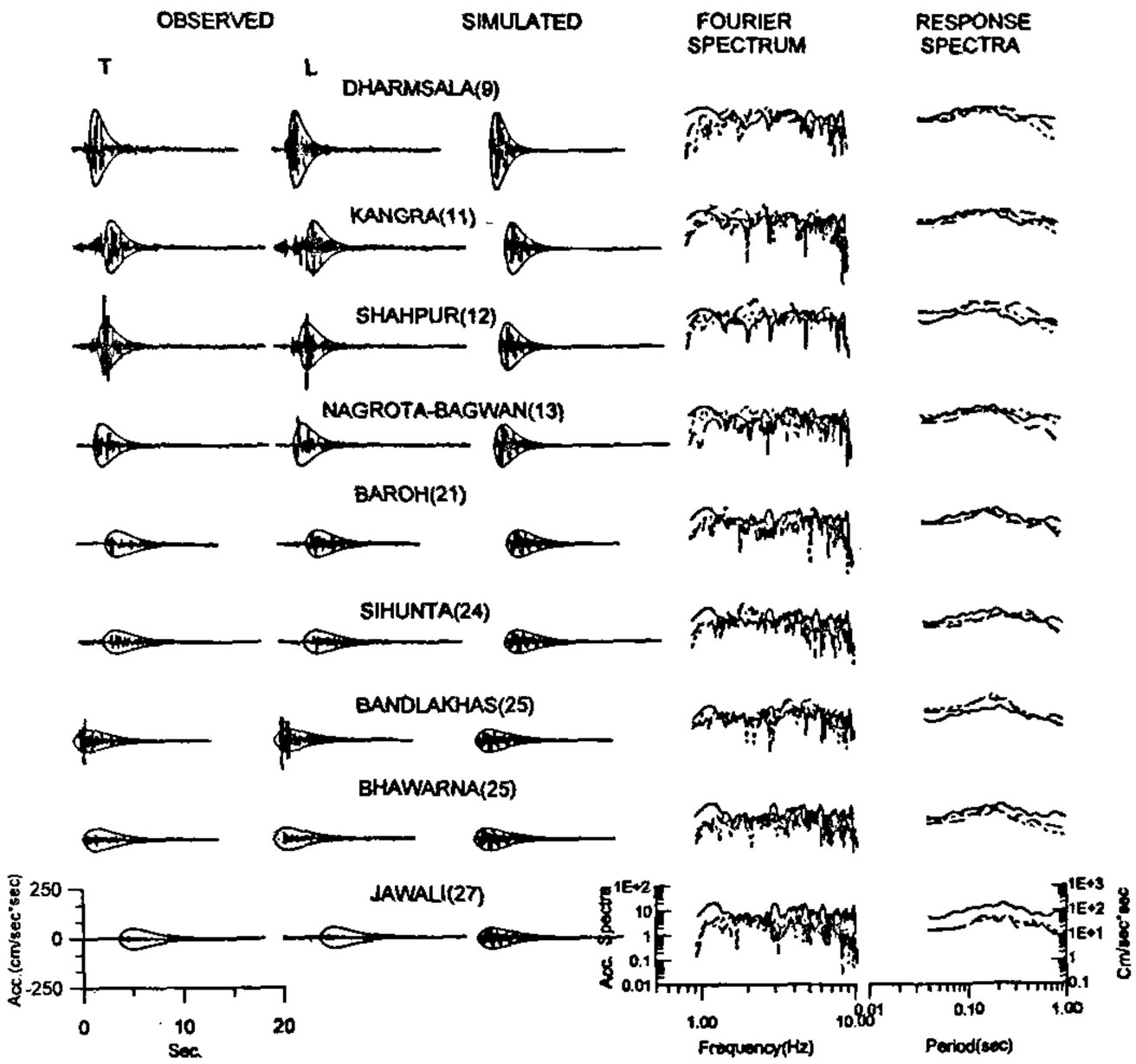

Figure 4. Observed (transverse and longitudinal horizontal components) accelerograms, simulated accelerograms, envelope functions, and corresponding Fourier and response spectra for the 1986 Dharmsala earthquake. The synthesized Fourier spectra are shown in continuous lines while long dash and small dash lines, respectively, indicate the Fourier spectra of transverse and longitudinal components of observed accelerograms. The same notation is used for response spectra. The numbers in brackets are hypocentral distances (km).

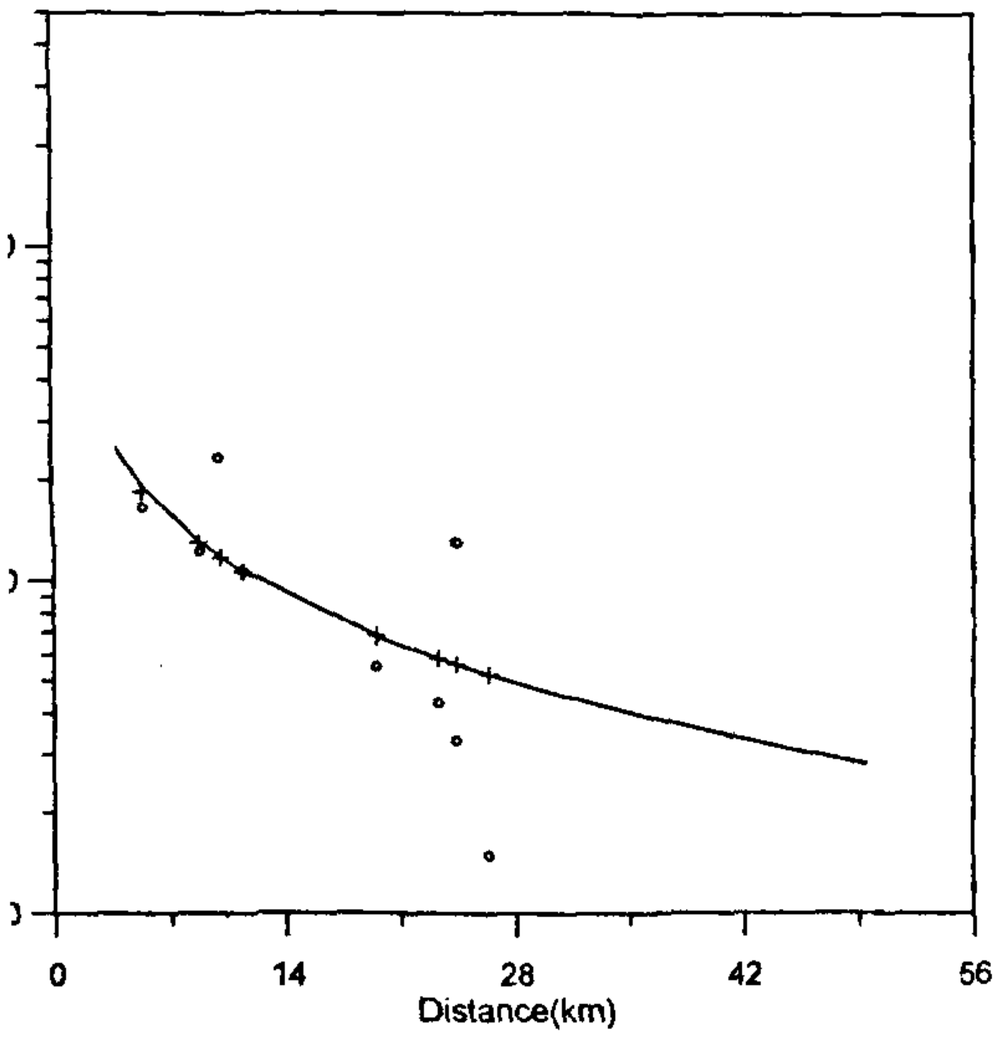

5. Comparison of observed acceleration (o) and synthesized ation (+) values for the 1986 Dharmsala earthquake. The ious curve indicates the regression used in the analysis.

the estimate obtained by the IMD and also by keeping it at the center of the fault plane (B). To understand the change in the shape of the envelope function with the change in the position of the epicenter, we have plotted the envelope waveforms from each of the 6 elements first separately and then together for the station at Bhatwari in Figure 6 *a* (corresponding to epicenter A) and Figure 6 *b* (corresponding to epicenter B). The final envelope functions in these figures show undulations which are the result of superposing the envelope functions from elemental earthquakes which are dependent on the direction of rupture propagation with reference to the azimuth of the recording station. The undulations are more with the epicenter at B than that at A due to the later arrivals of the individual envelope waveforms from the element 1 and 4 in the rear (Figure 3). On the other hand, with the epicenter at A, the composite envelope waveform is compressed by about 19% compared to the case for the epicenter at B. Furthermore, the peak amplitude is about 17% higher as compared to the case for the epicenter at B.

The results for all the 13 stations corresponding to the epicenters at A and B are shown in Figures 7 *a* and *b*. A

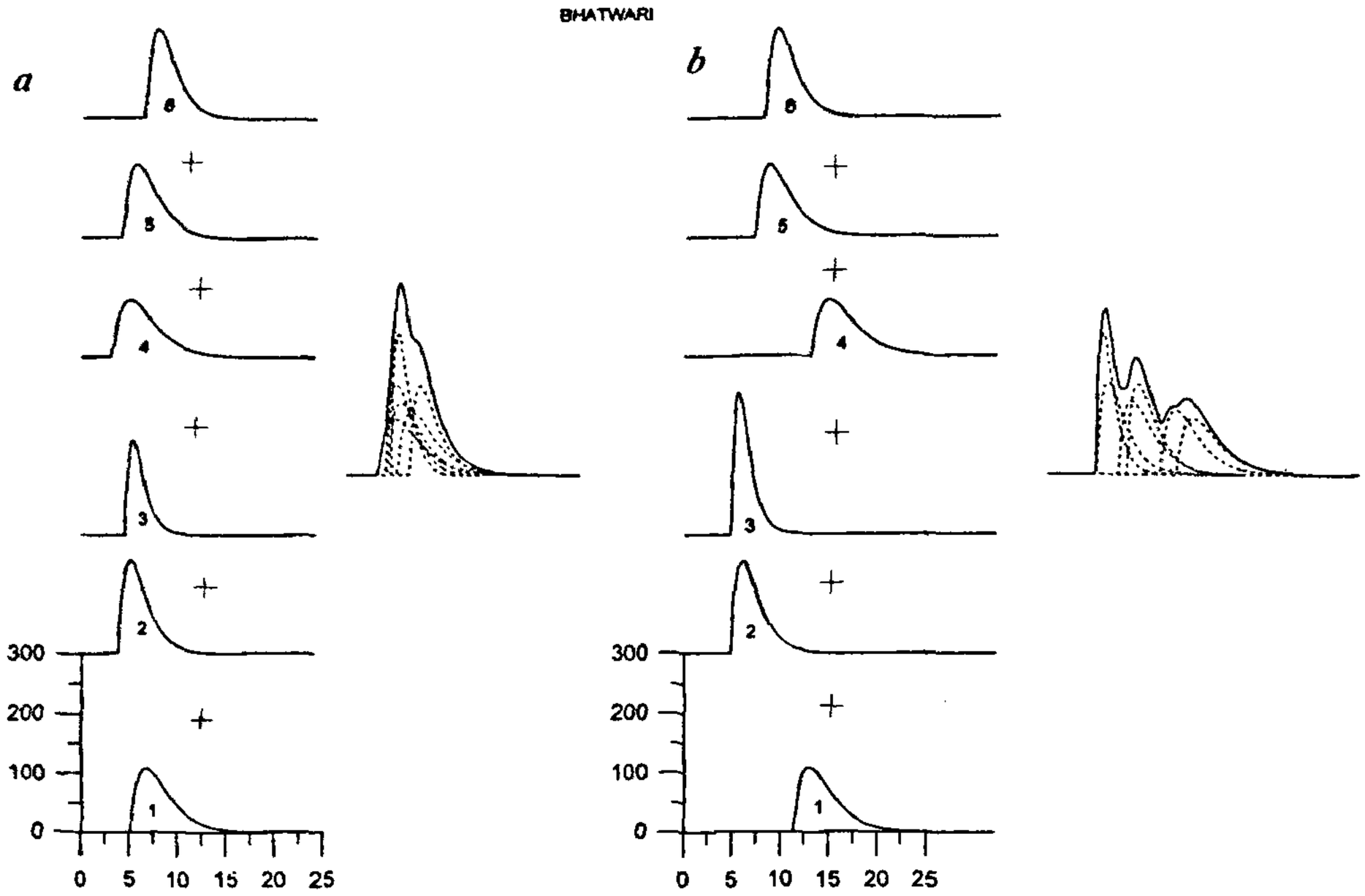

Figure 6 *a*, *b*. The envelope waveforms from the 6 elemental earthquake for the station at Bhatwari of the 1991 Uttarkashi earthquake with *a*, epicenter at A; *b*, epicenter at B. The number in the envelope waveforms indicates the element number (Figure 3) from which they are reaching.

rupture speed of 2.7 km/s has been used in the simulations. This speed is 0.9 times the shear wave speed of 3 km/s for the region[6]. A corner frequency of 0.02 Hz has been taken to be consistent with the magnitude (M_s 7) of the earthquake. The highest frequency in the synthetic accelerograms is again confined to be 10 Hz. The attenuation is taken into account as discussed above.

In Figure 7 *a* which corresponds to the epicenter at A, the synthetic accelerograms are having a satisfactory match with their empirical counterparts in terms of peak acceleration values, duration and frequency content at Bhatwari and Uttarkashi and in terms of peak acceleration and frequency content at Ghansiali and Koteshwar. At Barkot, the match is satisfactory in terms of the frequency content. At the remaining stations which are at larger distances the match is quite unsatisfactory, with the synthetic accelerograms being much more energetic for longer durations.

The matching of response spectra seen in Figure 7 *a* is good for the stations at Bhatwari, Uttarkashi and Ghansiali. The match for Barkot, Purola, Karanprayag and Koteshwar is satisfactory for shorter periods but for longer periods the synthetic response spectrum has larger energy. At these stations the observed peak amplitudes are close to the values obtained in the synthetic accelerograms which accounts for the better match of the response spectra at shorter periods. On the other hand, the larger durations of the synthetics cause the response spectra to be much higher than observed values. The stations at Tehri, Rudraprayag, Srinagar, Kosani and Almora show significantly smaller observed energies than in the synthetics. The above findings are also reflected in the Fourier spectra. The rmse of the synthetic with the observed response spectra at different intervals are shown in Table 2.

In Figure 7 *b* which corresponds to the epicenter at B, the synthetic accelerograms are having a satisfactory match with the observed accelerograms in terms of frequency content and peak ground acceleration values at Bhatwari, Uttarkashi, Barkot, Ghansiali and Koteshwar. The durations of the synthetics are more than that of the observed accelerograms at these stations. At the other stations the synthetic accelerograms are more energetic than those of the observed records, as was the case with the epicenter at A. The matching of response spectra is satisfactory at Bhatwari and Uttarkashi. The match is good for the shorter periods while for the longer periods the synthetic response spectrum has larger energy for stations at Barkot, Purola, Ghansiali and Koteshwar. At the remaining stations, the levels of the observed energies are smaller than those obtained for the synthetic

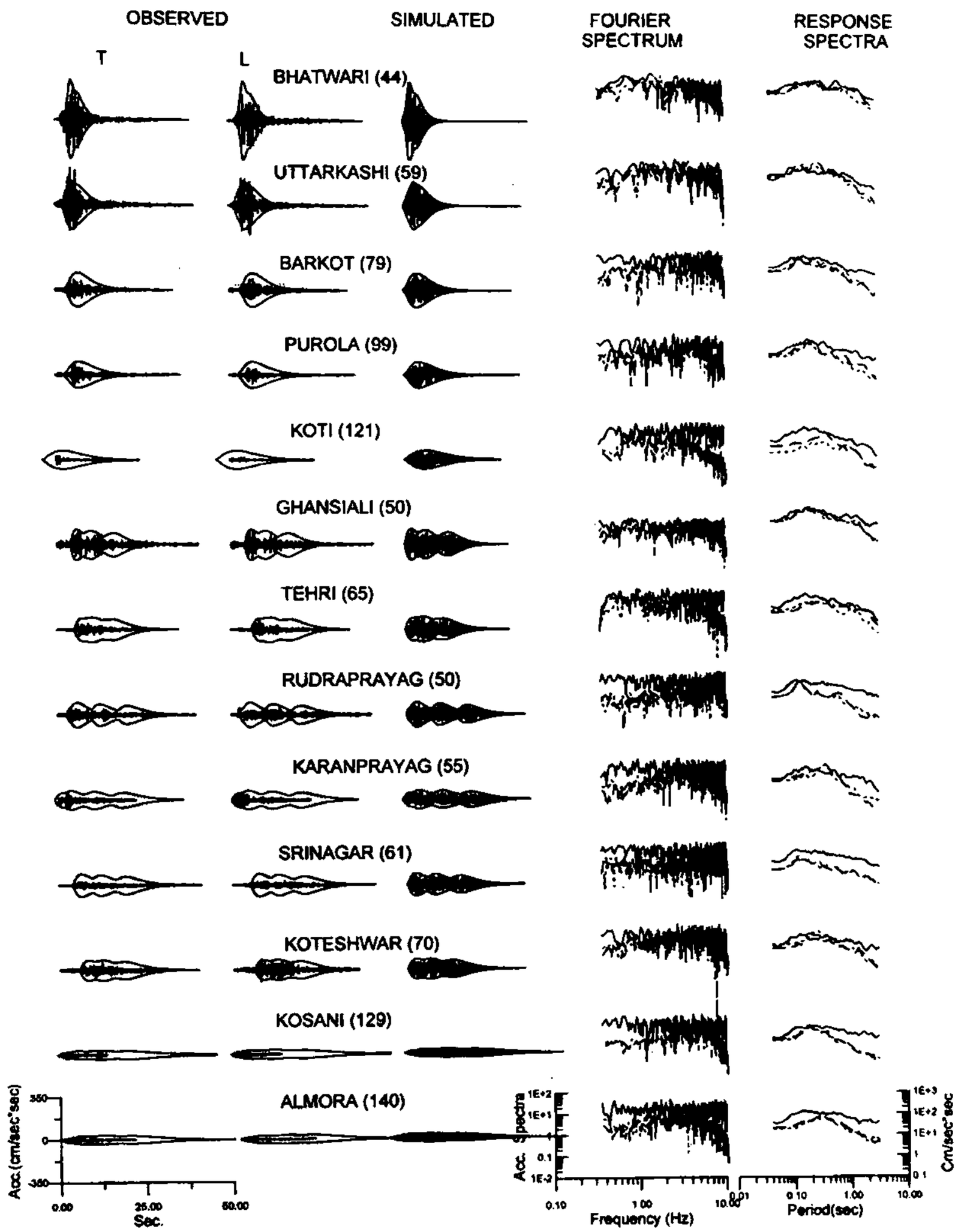

Figure 7 *a*. Observed (transverse and longitudinal horizontal components) accelerograms, simulated accelerograms, envelope functions, and corresponding Fourier and response spectra for the 1991 Uttarkashi earthquake. The synthesized Fourier spectra are shown in continuous lines while long dash and small dash lines respectively, indicate the Fourier spectra of transverse and longitudinal components of observed accelerograms. The same notation is used for response spectra. The numbers in brackets are hypocentral distances (km) with epicenter at A (Figure 3).

accelerograms. Table 3 gives the rmse between the synthetic and the observed response spectra values for different intervals.

A comparison of the peak ground acceleration values obtained in the observed and synthetic accelerograms respectively shown in Figure 7 *a* and *b* is displayed in Figure 8 *a* and *b*. It is observed that the matching of the peak ground acceleration values is sensitive to the choice of the epicenter. The peak ground acceleration values obtained in the synthetic accelerograms show a level of scatter that is smaller than that present in the empirical data. The scatter is smaller for the case of the epicenter at B. The decay rate follows closely the Abrahamson and Litehiser relation[19] used for scaling the individual envelope functions. The synthetic peak ground acceleration values are closer to this curve for the case

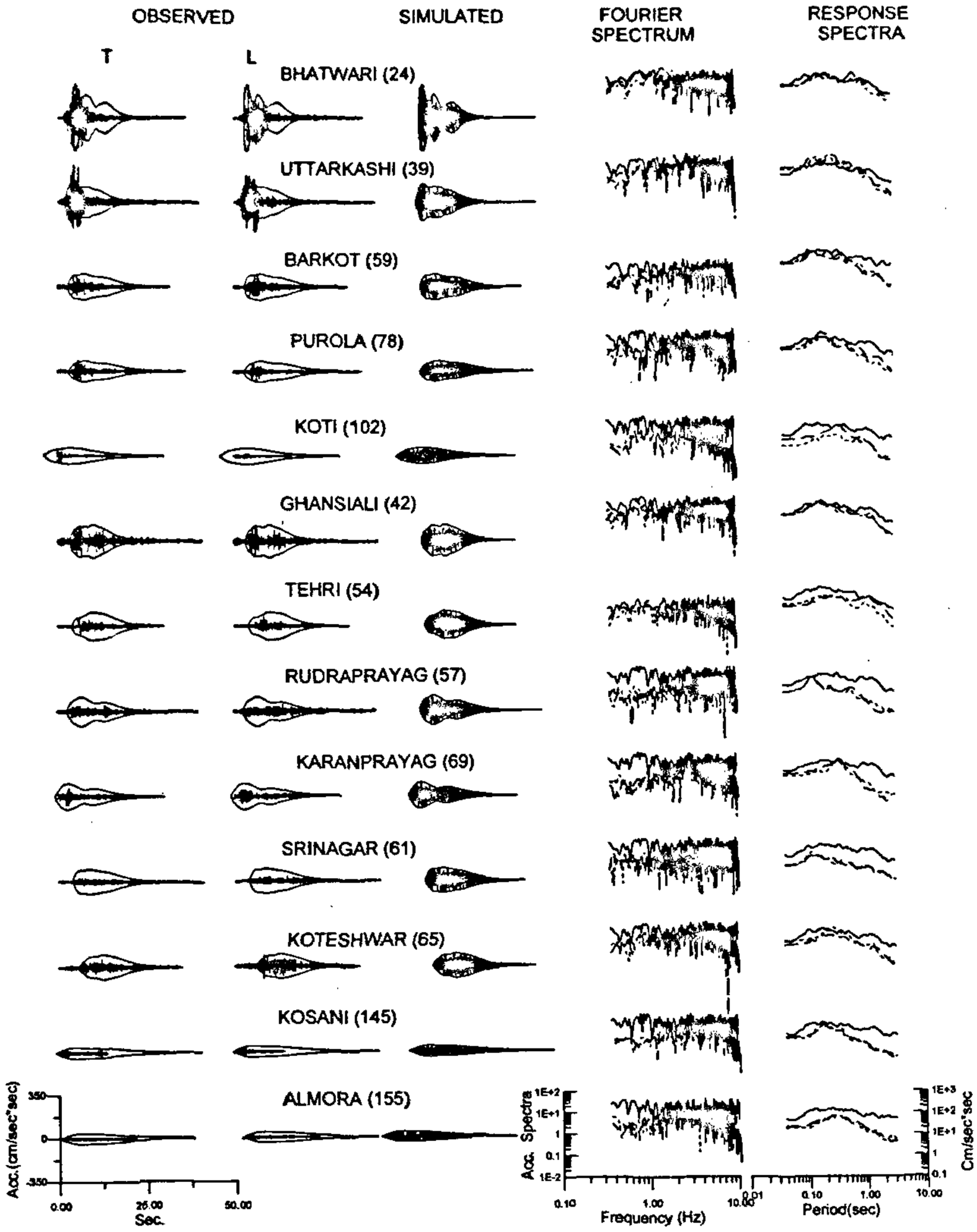

Figure 7 *b*. Observed (transverse and longitudinal horizontal components) accelerograms, simulated accelerograms, envelope functions, and corresponding Fourier and response spectra for the 1991 Uttarkashi earthquake. The synthesized Fourier spectra are shown in continuous lines while long dash and small dash lines respectively, indicate the Fourier spectra of transverse and longitudinal components of observed accelerograms. The same notation is used for response spectra. The numbers in brackets are hypocentral distances (km) with epicenter at B (Figure 3).

of the epicenter at B. As compared to the values obtained from the Abrahamson and Litehiser relation[19], the peak ground acceleration values for the case of the epicenter at B are about 5–10% higher and up to about 15% higher for the epicenter at A. There are a few stations at which the simulated values of the peak ground acceleration are lower in latter case. The estimation is expected to improve further with the use of regressions specific for Garhwal Himalaya as and when they become available.

Hypothetical great earthquake

We next estimate the accelerogram for the case of a M_w 8.5 earthquake at the Tehri site overlying the fault plane as shown in the Figure 9. The location and the

Table 2. The rms error of the synthetic with observed (T and L components) response spectra for the 1991 Uttarkashi earthquake (epicenter at A) for different intervals

Up to →	1s	1s	2s	2s	3s	3s
Station	T	L	T	L	T	L
Bhatwari	0.41	0.57	0.39	0.97	0.52	1.05
Uttarkashi	0.45	0.54	0.61	0.93	0.92	1.47
Barkot	0.97	0.79	1.67	1.17	2.76	2.67
Purola	1.07	1.52	1.43	2.56	2.04	3.33
Koti	1.98	4.16	2.51	4.08	2.99	4.11
Ghansiali	0.48	0.55	0.72	0.66	1.53	1.45
Tehri	1.47	1.11	1.34	1.16	1.28	1.54
Rudraprayag	2.02	2.47	5.56	3.52	5.66	4.43
Karanprayag	1.28	1.04	3.33	2.54	4.18	2.68
Srinagar	2.77	2.96	3.14	3.28	3.30	3.53
Koteshwar	1.08	0.73	1.15	0.98	2.44	1.92
Kosani	1.54	1.59	3.24	3.36	4.36	4.16
Almora	1.71	2.24	2.26	2.99	3.22	3.30

Table 3. The rms error of the synthetic with observed (T and L components) response spectra for the 1991 Uttarkashi earthquake (epicenter at B) for different intervals

Up to →	1s	1s	2s	2s	3s	3s
Station	T	L	T	L	T	L
Bhatwari	0.42	0.57	0.39	0.72	0.42	0.75
Uttarkashi	0.45	0.41	0.72	0.96	0.86	1.27
Barkot	1.10	0.74	2.04	1.25	3.01	2.80
Purola	0.78	1.31	1.56	2.90	2.03	3.33
Koti	1.69	3.72	2.48	3.84	3.97	4.39
Ghansiali	0.49	0.58	0.79	0.74	1.09	1.04
Tehri	1.96	1.84	1.79	1.86	1.75	2.31
Rudraprayag	3.37	3.79	9.23	5.76	9.08	6.12
Karanprayag	3.37	2.18	7.01	5.25	7.69	5.38
Srinagar	3.68	3.92	4.46	4.58	4.50	4.72
Koteshwar	1.36	0.88	1.67	1.51	2.55	2.07
Kosani	1.89	1.95	3.77	3.62	4.56	4.22
Almora	2.14	2.70	3.15	4.10	4.78	4.64

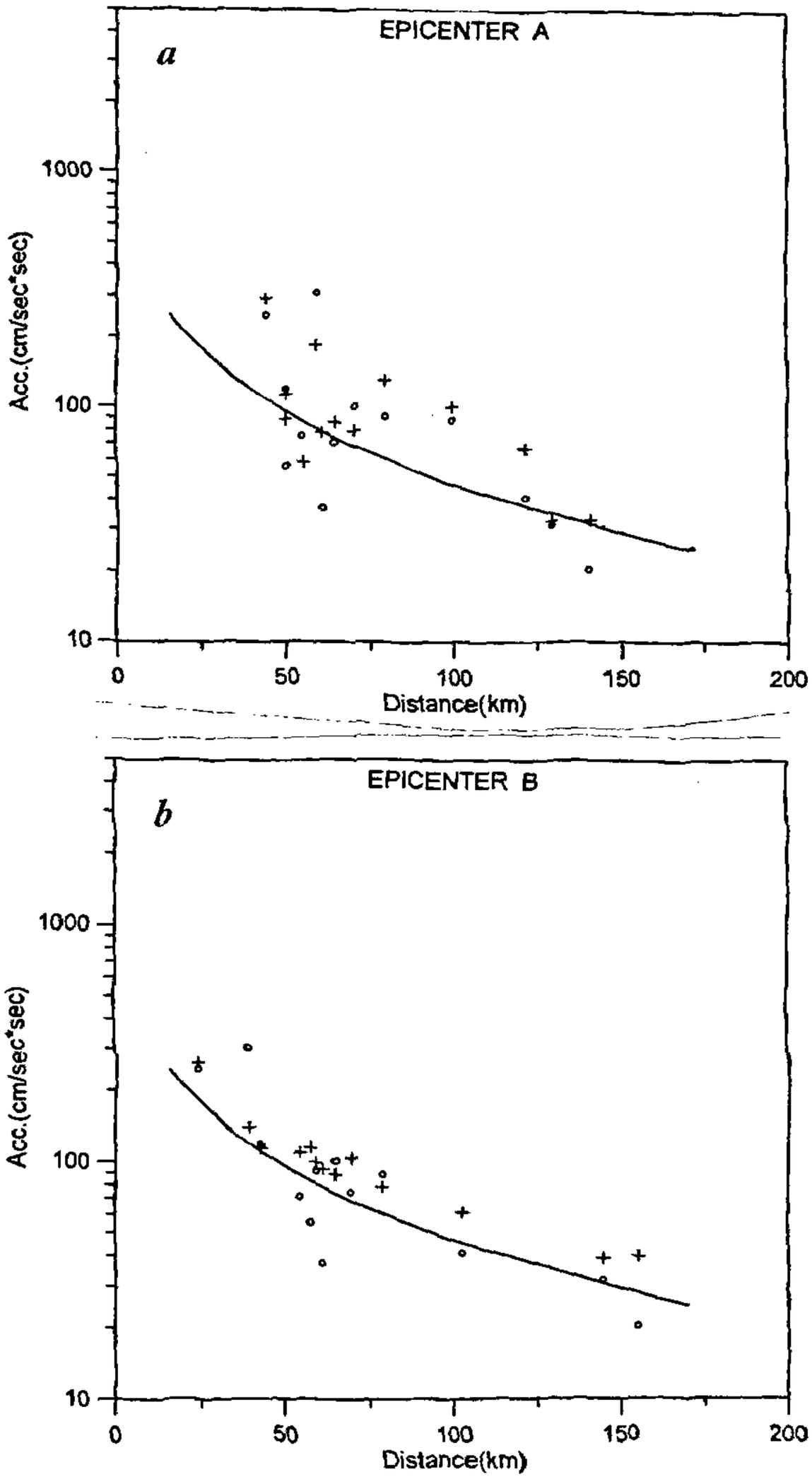

Figure 8 ***a***, ***b***. Comparison of observed acceleration (o) and synthesized acceleration (+) values for the 1991 Uttarkashi earthquake ***a***, for epicenter at A; ***b***, for epicenter at B. The continuous curve indicates the regression used in the analysis.

dimension of the fault plane are adapted from Yu *et al.*[7]. Three epicenters namely, A, B, and C have been considered. The element earthquake has a magnitude of 6.2 and 200 elements have been superposed. The rupture speed is 2.7 km/s. We have not included anelastic attenuation in this simulation.

The synthesized accelerograms and their corresponding spectra are shown in Figure 9. The largest peak ground acceleration of 536 cm/s^2 is observed for the case of the epicenter at A. Also this accelerogram has the shortest duration in keeping with the direction of rupture propagation. The accelerograms for epicenters at B and C show a comparatively longer duration and somewhat lower peak ground acceleration of 476–480 cm/s^2. The mean peak ground acceleration at Tehri for the epicenter at B, estimated using the composite source model is 494 ± 98 cm/s^2 for the E-W component and 970 ± 327 cm/s^2 for the N-S component while for the epicenter at A they are 542 ± 83 cm/s^2 and 778 ± 273 cm/s^2 respectively. We note that the composite source model incorporates the radiation pattern for the fault plane solution as well as variability of the rupture process by modelling it as a random distribution of sub-events over the main fault plane. The difference in the mean values of the peak ground acceleration for the E-W and N-S components is on account of the radiation pattern. The variability of peak ground acceleration is due to the rupture process model. In the present method,

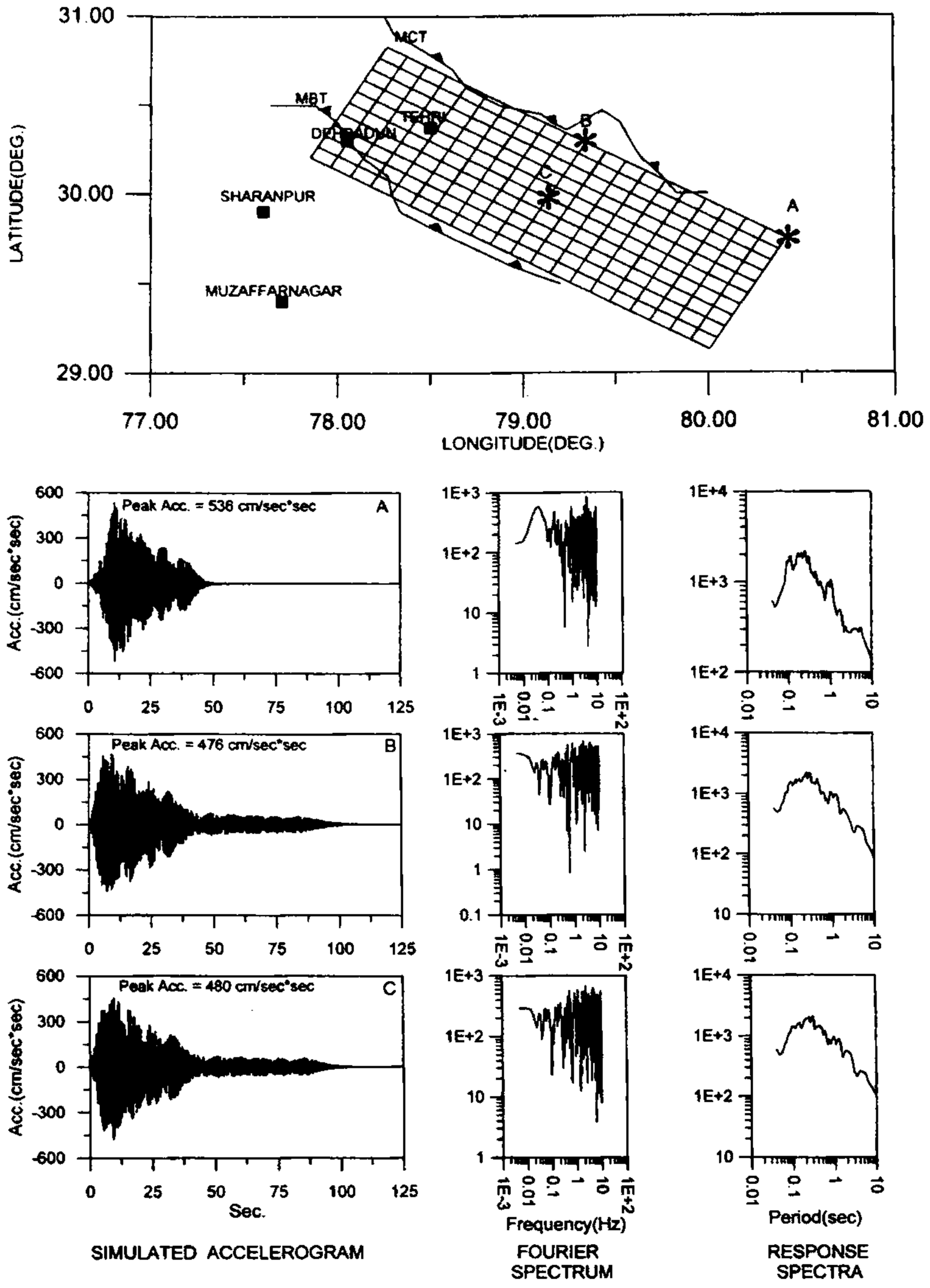

Figure 9. Source region of the hypothetical M_w 8.5 earthquake. The synthesized accelerograms and corresponding Fourier and response spectra at Tehri resulting from the hypothetical M_w 8.5 earthquake with epicenter at points A, B, and C are also shown.

both of these aspects have been ignored. Hence, the mean of the peak ground acceleration of the E–W and N–S components may be used for comparison. Thus, we note that the value obtained in the present work is about at the mean minus one standard deviation (s.d.) level obtained in the composite source simulation. Thus our results represent the lowest threshold of the expected peak ground acceleration level for the case of a great earthquake. This may be because we have used rather large sub-events which result in large epicentral distances from many of the sub-events to the site requiring specific consideration of the wave propagation effects.

In Figure 10, we compare the accelerograms for the epicenter at A with a particular set of synthetic accelerograms picked at random obtained by using the composite source model[7]. The fault model and the magnitude used are the same. The static stress drop is 63 bar and the stress parameter (dynamic stress drop) is

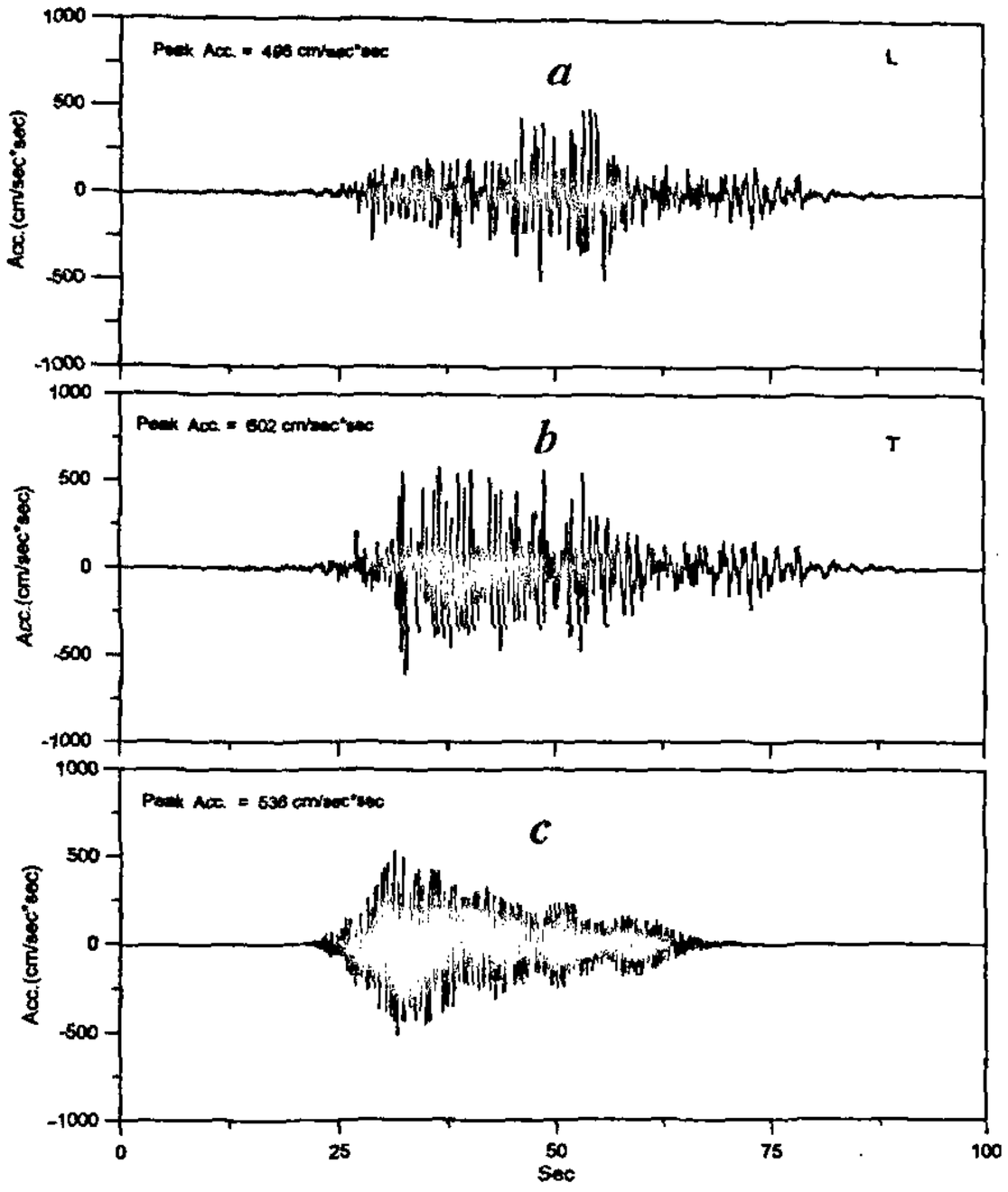

Figure 10 *a–c*. Comparison of accelerograms at Tehri for the epicenter at point A (Figure 9) obtained *a*, *b*, using the composite source model; **c**, using the proposed technique.

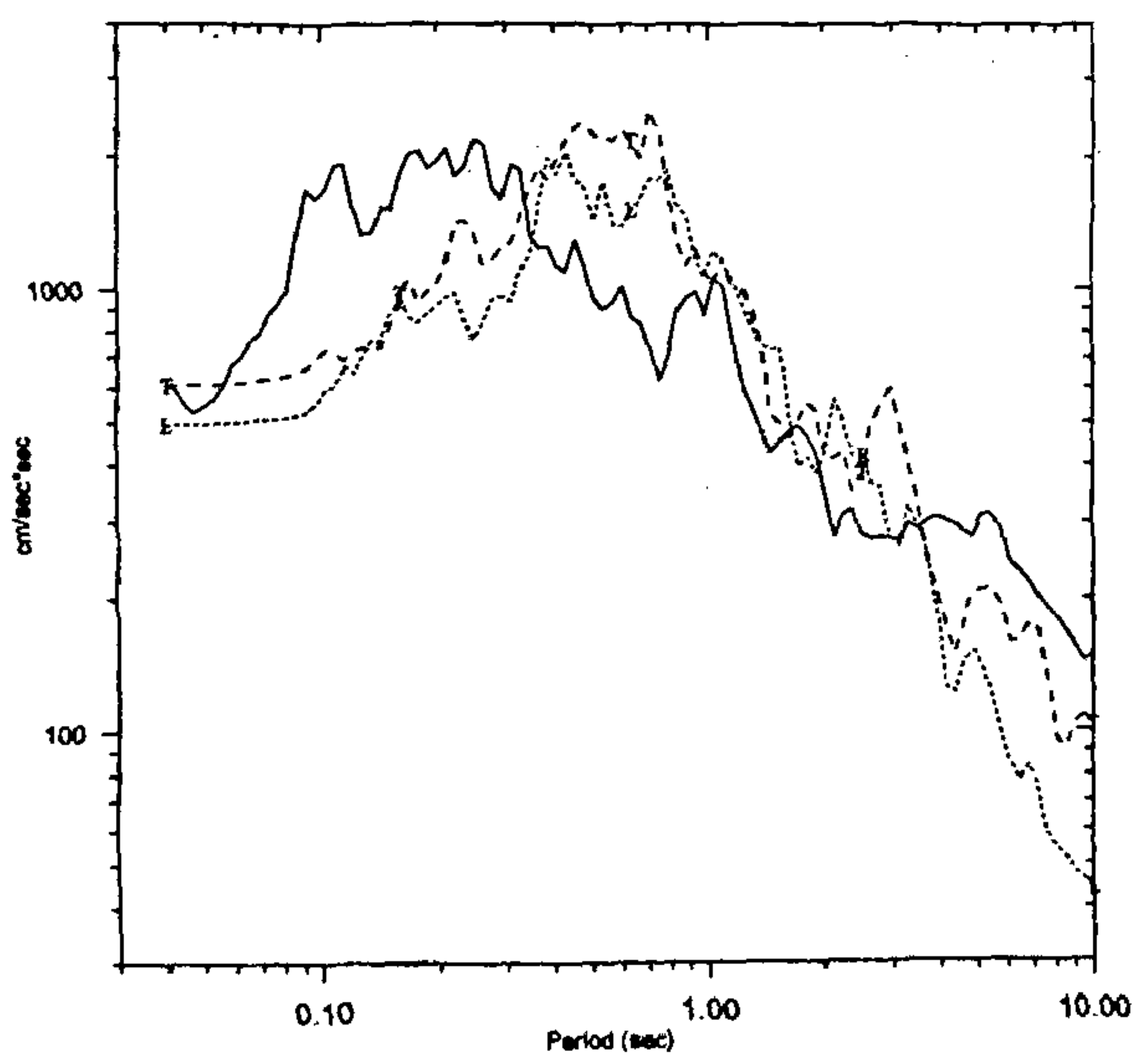

Figure 11. Comparison of response spectra (5% damping) of the accelerograms shown in Figure 10. The continuous curve corresponds to the response spectra obtained from the simulation by proposed technique.

100 bar. An appropriate velocity-Q structure was used[6]. The focal mechanism is of the thrust type[6]. The rupture speed was 2.7 km/s. The difference in the peak ground accelerations of the L (E–W) and T (N–S) components is due to the radiation pattern of the earthquake. The duration of the above accelerograms and the one obtained here are comparable. The accelerogram obtained by the present method is richer in higher frequencies as compared to the accelerograms obtained using the composite source model. Also the stronger peaks (500 cm/s^2) last for about 20 s in the T component and 10 s in the L component. In our case, they last for about 10 s. Our simulation also lacks various wave phases, e.g. the long period surface waves which have extended the duration of the accelerograms in the composite source model as compared to the accelerogram obtained by us. We also do not simulate the pre-shear wave phases which can be seen in the accelerograms obtained using the composite source model. However, the mean of peak ground acceleration values of the L and T components obtained in the composite source model in this particular realization is 549 cm/s^2 which is very close to the value of 536 cm/s^2 estimated in this paper. The response spectra are compared in Figure 11. They are fairly well-matched in terms of the shape for the period range 0.9–4 s for the T component. The higher energy present in the shorter periods in the present simulation as compared to that obtained in the accelerogram calculated using composite source model is due to not having included the anelastic attenuation in the wave propagation in our estimation. The match for the short periods on the average can be improved by accounting for attenuation. However, the deficiency of energy in the 0.4–0.9 s range will remain. On the other hand, there is larger energy in the period longer than 3s. Both of these effects seem to be related to the way the main fault has been discretized. Using smaller sub-events may correct this situation. The spectral acceleration values are in general lower by up to 25% in the period range of 1.0–3.0 s as compared to the average composite source estimates reflecting the similar observations in the case of peak ground acceleration. We consider the estimates obtained using the composite source model as reliable and realistic having taken into account in the model various aspects of the processes in detail. While the method in this paper is found to be quite successful up to M_s 7, it needs further improvement for better estimation of the accelerograms for the case of great earthquakes.

Discussion and conclusions

We have presented here the application of a very simple and fast method for obtaining synthetic accelerograms and the corresponding response spectra first presented by Khattri[16]. Its suitability has been demonstrated by

successfully modelling the accelerograms from two Himalayan earthquakes. Also the accelerogram from a hypothetical great earthquake has been synthesized and compared with the accelerogram obtained using the composite source model and was found to be well matched.

The quality of modelling of the empirical accelerograms deteriorates as the distance increases. This may be attributed to increasing complexities in the geological conditions along the wave path. Sophisticated modelling procedures which can take into account the complexities of the geological conditions at such distances will be needed for more precise results.

The method presented here estimates the lower bound of the hazard parameter peak ground acceleration and response spectra for the case of great earthquakes which is 1 s.d. lower than the mean values of the parameters of hazard evaluated using the comprehensive composite source model. However, the technique in its present form is found to be quite suitable for the earthquakes up to moderate magnitudes (~ 7) and at relatively smaller epicentral distances.

The advantage of the proposed method not only lies with its speed of implementation but also because it does not require specification of the detailed model of the velocity-Q structure, the fault plane solution, or the stress parameter. Therefore it can encompass a wide range of such parameters in the estimation process. This will be helpful in dealing with regions where such detailed knowledge is not currently available. While the above are strong points of the method for a first order estimation of the strong motion characteristics, they appear to be just the opposite in case a detailed and more precise estimation is required. We propose to extend the scope of this method by incorporating the issue of variability of the earthquake processes and wave propagation effects by introducing stochastic variability in the rupture process, as well as in the attenuation and the envelope functions, thereby making the model more in tune with the natural phenomena. Even with such enhanced features in the model the method will remain computationally very efficient. Because of the speed of the implementation, this method can find application also in preparing a wide range of scenarios as well as, on the basis of simulations, evolving uniform probability response spectra for various regions.

1. Chang, M., Kwiatkowski, J., Nau, R., Oliver, R. and Pister, K., *Earthquake Eng. Struct. Dyn.*, 1982, **10**, 651–662.
2. Nau, R., Oliver, R. and Pister, K., *Bull. Seismol. Soc. Am.*, 1982, **72**, 615–636.
3. Jurkevics, A. and Ulrych, T., *Bull. Seismol. Soc. Am.*, 1978, **68**, 781–801.
4. Westermo, B., *Earthquake Eng. Struct. Dyn.*, 1992, **21**, 743–756.
5. Zeng, Y., Anderson, J. and Yu, G., *Geophys. Res. Lett.*, 1993, **21**, 725–728.
6. Khattri, K. N., Zeng, Y., Anderson, J. G. and Brune, J., *J. Himalayan Geol.*, 1994, **5**, 163–191.
7. Yu, G., Khattri, K. N., Anderson, J. G., Brune, J. N. and Zeng, Y., *Bull. Seismol. Soc. Am.*, 1995, **85**, 31–50.
8. Hartzell, S., *Geophys. Res. Lett.*, 1978, **5**, 1–4.
9. Irikura, K., Proc. 7th Japan Earthquake Engineering Symp., 1986, 151–156.
10. Irikura, K. and Kamae, K., *Annalidi Geopfisica*, 1994, **XXXVII**, 1721–1743.
11. Dan, K., Watanabe, T. and Tanaka, T., *J. Struct. Construct. Eng.*, 1989, **403**, 35–44.
12. Dan, K., Watanabe, T. and Tanaka, T., *J. Struct. Construct. Eng.*, 1990, **407**, 23–33.
13. Dan, K., Tanaka, T. and Watanabe, T., *J. Struct. Construct. Eng.*, 1987, **373**, 50–62.
14. Hutching, L. J. and Wu, F. T., *J. Geophys. Res.*, 1990, **95**, 1187–1224.
15. Midorikawa, S., *Tectonophysics*, 1993, **218**, 287–295.
16. Khattri, K. N., National Seminar on Recent Advances in Seismology, Department of Mathematics, M.D. University, Rohtak, January 15–16, 1998.
17. Kameda, H. and Sugito, M., Proc. 6th Japan Earthquake Engineering Symp., 1978, pp. 41–48.
18. Peng, K. Z., Wu, F. T. and Song, L., *Earthquake Eng. Struct. Dyn.*, 1985, **13**, 337–350.
19. Abrahamson, N. A. and Litehiser, J. J., *Bull. Seismol. Soc. Am.*, 1989, **79**, 549–580.
20. Dinesh Kumar, Teotia, S. S. and Khattri, K. N., *Curr. Sci.*, 1997, **73**, 543–548.
21. Das, J. D. and Chandrasekaran, A. R., *J. Geol. Soc. India*, 1993, **41**, 417–430.
22. Gupta, S. C., Singh, V. N. and Ashwani Kumar, *Phys. Earth Planet Inter.*, 1995, **87**, 247–253.

ACKNOWLEDGEMENTS. We appreciate the critical and constructive comments by Prof. V. K. Gaur. D.K. and S.S.T. are thankful to KUK and DST for the support of this research. S.S.R. is indebted to NGRI for supporting this investigation.

Received 13 October 1998; revised accepted 11 December 1998